The Structure of $PO(OPF_2)_3$ in the Gaseous and Crystalline Phases *

David W. H. Rankin, Alexander J. Blake, Martin J. Davis, E. A. V. Ebsworth, and Alan J. Welch
Department of Chemistry, University of Edinburgh, West Mains Road, Edinburgh EH9 3JJ

The structure of $P'O'(OPF_2)_3$ has been determined in the gas and solid phases by electron diffraction and *X*-ray crystallography respectively. The compound was found to undergo an irreversible, topotactic phase change at *ca.* 77 K and, accordingly, the single-crystal structure for the lower-temperature form was determined. *X*-Ray powder diffraction was used to study both solid forms and investigate the transition between them. The principal parameters (r_a) found in the gas phase were r(P'=O') 1.401(10), r(P'–O) 1.590(9), r(O–P) 1.576(25), r(P–F) 1.581(10) Å, and O–P'–O 102.8(7), O–P–F 98.3(6), and F–P–F 96.4(14)°. The conformations in the two phases are considerably different. Overall, a general flattening of the molecule is observed on going to the crystalline phase, due to an increase in the O–P'–O angle and changes in the P'–O–P–F dihedral angles. There was also a lengthening of r(P'=O') by about 0.08 Å to 1.478(9) Å, which may be associated with short intermolecular contacts, P=O • • • P, of 2.88 and 3.14 Å.

The compound $PO(OPF_2)_3$ has previously been prepared[1] and some of its properties have been studied.[1,2] The reported melting point of 254 K is considerably higher than might be expected by comparison with similar compounds. The compound $P(OPF_2)_3$ has only one fewer oxygen atom yet its melting point of 165 K is far lower. This suggests the possibility of significant intermolecular interactions in the solid, supported by the observation that $PO(OPF_2)_3$ readily crystallises into rod-like microcrystals. Further evidence comes from observation of the frequency of the phosphoryl stretching band in the i.r. spectrum. In the crystalline phase this band is found at 1 258 cm^{-1}, 87 cm^{-1} lower than in the gas phase and 40 cm^{-1} lower than for the amorphous solid. This suggests that the intermolecular interactions involve the phosphoryl group in some manner, though exactly how is not clear.

The determination of the crystal structure should give a much clearer idea of the nature of the intermolecular interaction and comparison with the gas-phase structure would give some insight into the intramolecular structural changes which occur as the molecules associate in the crystalline phase. The gas-phase structure is also of interest as very little structural work has been done on compounds containing OPF_2 groups.[3–7] Furthermore, since this compound has potential as a tridentate ligand for co-ordination to metals, the structure of the free ligand would be useful for comparison with structures of complexes containing it. We have therefore studied the structure of $PO(OPF_2)_3$ in both gaseous and crystalline phases.

Experimental

A sample of $PO(OPF_2)_3$ was prepared by reaction of pure orthophosphoric acid with $S(PF_2)_2$ and purified by fractional condensation using standard vacuum-line techniques.[1]

Electron Diffraction.—The electron diffraction data were collected on Kodak Electron Image plates using the Edinburgh/Cornell diffraction apparatus.[8] Two plates were used at each camera distance (128, 286 mm) with an accelerating potential of *ca.* 45 kV. The plates were traced using a Joyce-Loebl microdensitometer[9] at the S.E.R.C. Daresbury Laboratory, and the data were transferred to an Amdahl-V7 computer on which the rest of the analysis was performed using standard data-reduction[9] and least-squares refinement[10] programs and the scattering factors of Schäfer *et al.*[11] Weighting functions, correlation parameters, and scale factors are given in Table 1.

Throughout the refinements of the structure it was assumed that only one conformer, of C_3 symmetry, was present. Thus the structure could be defined by 10 structural parameters, the distances P'=O', P'–O, O–P, and P–F, the angles OP'O, P'OP, OPF, and FPF, and the twist angles about the P'–O and O–P bonds (P' denotes central, quinquevalent phosphorus, O' denotes double bonded oxygen). The twist angles are defined to be zero when P eclipses O' and when the bisector of the FPF angle eclipses P' respectively). Initial values were assigned to the parameters by reference to similar compounds. Values for the two twist angles were difficult to assign and were set initially to those found in the crystal structure. The distances P–F, P'–O, and O–P and angles FPF and OPF were refined and then more accurate starting values for the twist angles were determined by a series of refinements in which values of the two twist angles were varied in regular steps over their entire possible ranges.

Table 1. Weighting functions, correlation parameters, and scale factors for $PO(OPF_2)_3$

Camera height (mm)	Δs	$s_{min.}$	s_{w1}	s_{w2}	$s_{max.}$	Correlation parameter	Scale factor, k	Wavelength (Å)
	Å^{-1}							
128.3	0.4	6.0	8.0	30.0	35.2	0.4660	0.659(11)	0.056 87
285.7	0.2	2.0	4.0	12.2	14.4	0.4693	0.692(8)	0.056 87

Table 2. Molecular parameters (r_a) for gaseous $PO(OPF_2)_3$ (distances in Å, angles in °)

p_1(P'=O')	1.401(10)
p_2(mean P–O)[a]	1.583(11)
p_3(diff. P–O)[a]	−0.014(30)
p_4(P–F)	1.581(10)
p_5(OP'O)	102.8(7)
p_6(P'OP)	132.0(16)
p_7(P'–O twist)[b]	126.6(12)
p_8(O–P twist)[b]	127.1(16)
p_9(OPF)	98.3(6)
p_{10}(FPF)	96.4(14)

[a] For definition see text. [b] Positive clockwise in direction from first to second atom. For definition of zero see text.

* Tris(difluorophosphino-oxo)phosphine oxide.

Supplementary data available: see Instructions for Authors, *J. Chem. Soc., Dalton Trans.*, 1989, Issue 1, pp. xvii–xx.

Thus a matrix of values of the R factor, R_G, as a function of the two independent angles was obtained. Conformations which gave the lowest values of R_G were then studied more closely. Some could be dismissed immediately as they involved unrealistic geometric parameters, but the remainder were refined further until one structure showed a much better fit than any of the others.

After all geometrical parameters (Table 2) had been refined, attempts were made to refine amplitudes of vibration. This proved difficult at first because of a number of strong correlations (Table 3), particularly between the P–O and P–F distances. This is due to the overlap of these peaks in the radial distribution curve (Figure 1). It was found necessary to fix most of the geometrical parameters first, though they were allowed to refine again after refining the most important amplitude parameters. The values of all amplitudes of vibration, except those for the long F · · · F distances, were eventually refined, although it was necessary to constrain some of them in groups such that all values within any one group were equal (Table 4). Since the two types of single P–O bond were of very similar length they were represented by a mean and a difference (defined to be positive when the bond to the PF_2 group was longer than that to the central phosphorus atom). The mean was then better determined than were the individual distances, most of the uncertainty being associated with the difference parameter. The final value of R_G was 0.065, which indicates a very good fit and thus suggests that the original assumptions made about the structure are valid. The experimental and final difference molecular scattering curves are shown in Figure 2 and the final atom co-ordinates are given in Table 5. Figure 3 shows the gas-phase structure.

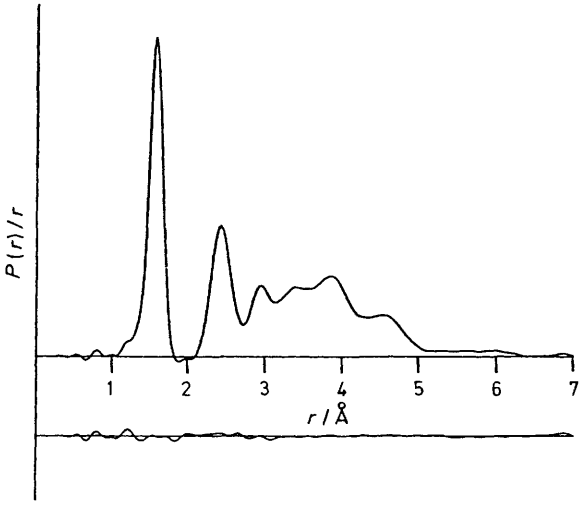

Figure 1. Observed and final difference radial-distribution curves, $P(r)/r$, for $PO(OPF_2)_3$. Before Fourier inversion, the data were multiplied by $s \cdot \exp[(-0.002\ s^2)/(Z_P - f_P)(Z_F - f_F)$

Single-crystal Study.—A sample was sealed in a Pyrex capillary tube and a crystal was grown by a modification of the

Table 3. Least-squares correlation matrix (×100) for the gas-phase study of $PO(OPF_2)_3$. All elements with absolute value <50 have been removed

p_3	p_4	p_5	p_6	p_7	p_8	p_9	p_{10}	u_5	u_6	u_{14}	u_{15}	k_1	k_2	
												−55	−57	p_1
78	−99		−92		57			64		60				p_2
	−76	65	−62							61				p_3
			91		−57			−64		−62				p_4
				73			−81		−63					p_5
								−71	53					p_6
						52	−75							p_7
						−82	62	65		64				p_8
							−58			−59				p_9
									66					p_{10}
												57		u_1
											−60			u_{11}
													56	k_1

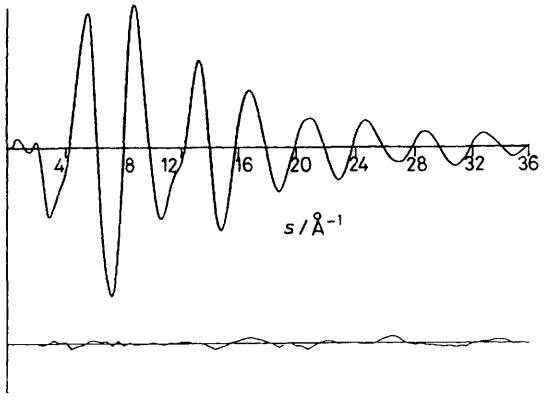

Figure 2. Observed and final weighted difference combined molecular-scattering intensities for $PO(OPF_2)_3$

Table 4. Interatomic distances (r_a/Å) and amplitudes (u/Å) for gaseous $PO(OPF_2)_3$

	Distance	Amplitude		Distance	Amplitude
d_1(P–F)	1.581(10)	0.053(1)	d_{16}[F(5) · · · O(2)]	4.814(19)	
d_2(P′–O′)	1.401(10)	0.048 (tied to u_1)	d_{17}[F(6) · · · O(2)]	4.673(11)	
d_3(P′–O)	1.590(9)	0.053 (tied to u_1)	d_{18}[F(5) · · · O(7)]	4.584(25)	0.221(19)
d_4(P–O)	1.576(25)	0.053 (tied to u_1)	d_{19}[F(5) · · · O(11)]	4.491(24)	
d_5(P′ · · · P)	2.893(8)	0.104(8)	d_{20}[F(6) · · · O(7)]	3.535(19)	
d_6[F(5) · · · F(6)]	2.357(31)		d_{21}[F(6) · · · O(11)]	3.290(37)	
d_7[F(5) · · · O(3)]	2.389(12)	0.076(8)	d_{22}[P(4) · · · F(9)]	5.445(22)	
d_8(O′ · · · O)	2.532(12)		d_{23}[P(4) · · · F(10)]	3.625(40)	0.239(17)
d_9(O · · · O)	2.485(13)		d_{24}[P(4) · · · F(13)]	4.429(18)	
d_{10}[P(1) · · · F(5)]	3.971(9)		d_{25}[P(4) · · · F(14)]	3.327(30)	
d_{11}[P(1) · · · F(6)]	3.365(9)	0.141(9)	d_{26}[F(5) · · · F(9)]	5.996(22)	0.200 (fixed)
d_{12}(P · · · O′)	3.910(10)		d_{27}[F(5) · · · F(10)]	4.297(54)	0.200 (fixed)
d_{13}[P(4) · · · O(7)]	3.716(16)	0.113(12)	d_{28}[F(5) · · · F(14)]	4.655(29)	0.200 (fixed)
d_{14}[P(4) · · · O(11)]	3.022(23)		d_{29}[F(6) · · · F(10)]	2.464(42)	0.200 (fixed)
d_{15}(P · · · P)	3.965(22)	0.213(25)			

Table 5. Atom co-ordinates for gaseous $PO(OPF_2)_3$

Atom	*x*	*y*	*z*
P(1)	0.000 00	0.000 00	0.000 00
O(2)	0.000 00	0.000 00	1.400 91
O(3)	1.434 88	0.000 00	−0.685 08
P(4)	2.087 79	0.939 64	−1.769 37
F(5)	3.458 00	0.169 49	−1.943 96
F(6)	1.383 20	0.335 18	−3.049 71
O(7)	−0.717 44	−1.242 64	−0.685 08
P(8)	−0.230 14	−2.277 89	−1.769 37
F(9)	−1.582 21	−3.079 46	−1.943 96
F(10)	−0.401 33	−1.365 48	−3.049 71
O(11)	−0.717 44	1.242 64	−0.685 08
P(12)	−1.857 64	1.338 26	−1.769 37
F(13)	−1.875 79	2.909 97	−1.943 96
F(14)	−0.981 87	1.030 30	−3.049 71

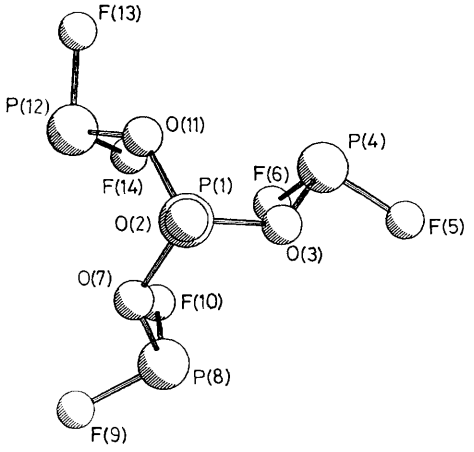

Figure 3. The gas-phase structure of $PO(OPF_2)_3$, viewed along the C_3 symmetry axis

procedure described previously:[12] the capillary tube was positioned above the cold stream and parallel to it, and crystal growth was induced by slowly tilting the tube into the cold stream. Oscillation and Weissenberg photography showed the crystal to be hexagonal, but on transfer (in liquid nitrogen) to the diffractometer a phase transformation occurred to yield a crystal in the trigonal system.

Crystal data. $F_6O_4P_4$, M = 301.88, trigonal, a = 12.874(4), c = 9.239(21) Å, U = 1 326 Å^3 (by least-squares refinement on diffractometer angles for 25 automatically centred reflections with θ = 17–18°, $\bar{\lambda}$ = 0.710 69 Å), T = 158 K, space group $P\bar{3}c1$, Z = 6, D_c = 2.268 g cm^{-3}, $F(000)$ = 876. Colourless, cylindrical crystal 0.4 × 0.4 × 0.5 mm, μ(Mo-K_α) = 0.833 mm^{-1}.

Data collection and processing. CAD4 diffractometer, T = 158 K, ω–2θ mode with ω scan width (0.80 + 0.35 tan θ)°, graphite-monochromated Mo-K_α radiation, 4 242 reflections measured ($\theta_{max.}$ = 30°, $\pm h, k, l$), 1 295 unique (R_{int} = 0.0149), giving 1 287 with $F > 2\sigma(F)$ for use in all calculations, no significant crystal movement or decay, no absorption correction.

Structure analysis and refinement. Direct methods[13] yielded the positions of all atoms. Full-matrix least-squares refinement[14] with all atoms anisotropic except O(5), whose anisotropic thermal parameters refined to unrealistic values. There appears to be slight disorder affecting the chain of molecules containing P(1) and O(1), but extensive efforts to model the disorder were unsuccessful. At final convergence, R, R' = 0.0993, 0.1507, S = 1.221, with the weighting scheme w^{-1} = $\sigma^2(F) + 0.000\,75F^2$ giving satisfactory agreement analyses. Molecular geometry calculations utilised CALC[15] and illustrations were produced using ORTEP[16] and PLUTO.[17] Fractional co-ordinates are given in Table 6, and derived molecular geometry parameters in Table 7.

Additional material available from the Cambridge Crystallographic Data Centre comprises thermal parameters.

Table 6. Fractional co-ordinates of atoms of crystalline $PO(OPF_2)_3$ with standard deviations in parentheses

Atom	*x*	*y*	*z*
Molecule 1			
O(1)	0.333 33	0.666 67	0.620 3(20)
P(1)	0.333 33	0.666 67	0.466 70
P(2)	0.236 6(3)	0.445 12(24)	0.284 8(6)
F(1)	0.122 4(7)	0.431 8(7)	0.200 0(12)
F(2)	0.167 7(10)	0.334 6(9)	0.389 6(15)
O(2)	0.240 5(6)	0.540 7(6)	0.404 5(11)
Molecule 2			
P(3)	0.666 67	0.333 33	0.030 0(6)
P(4)	0.550 61(25)	0.437 35(25)	−0.149 0(6)
F(3)	0.646 8(8)	0.547 6(7)	−0.231 7(11)
F(4)	0.509 4(10)	0.507 4(10)	−0.044 5(14)
O(3)	0.666 67	0.333 33	0.190 5(15)
O(4)	0.643 3(7)	0.432 1(7)	−0.030 0(11)
Molecule 3			
P(5)	0.0	0.0	−0.077 0(7)
P(6)	0.214 99(22)	0.153 49(23)	0.100 0(7)
F(5)	0.254 2(7)	0.073 8(8)	0.184 0(11)
F(6)	0.329 5(7)	0.216 0(7)	0.000 3(11)
O(5)	0.0	0.0	−0.236 7(15)
O(6)	0.127 3(6)	0.046 6(6)	−0.016 5(10)

Table 7. Comparison of crystal and gas-phase structural parameters for $PO(OPF_2)_3$ (distances in Å, angles in °)

	Crystal			
	Molecule 1	Molecule 2	Molecule 3	Gas phase
r(P′=O′)	1.419(11)	1.482(9)	1.475(9)	1.401(10)
r(P′–O)	1.566(9)	1.548(10)	1.541(9)	1.590(9)
r(O–P)	1.636(10)	1.649(10)	1.665(10)	1.576(25)
r(P–F)	1.598(11)	1.541(11)	1.559(11)	1.581(10)
	1.577(14)	1.583(13)	1.575(10)	
O–P′–O	107.3(4)	107.9(5)	107.6(5)	102.8(7)
P′–O–P	138.4(6)	135.6(6)	134.9(6)	132.0(16)
φ(O′–P′–O–P)[a]	−130.5(9)	−129.0(8)	126.2(8)	126.6(12)[b]
φ(P′–O–P–F)[a]	−128.0(9)	−131.8(9)	134.5(8)	175.3(17)[b]
	134.1(9)	130.8(9)	−129.1(8)	78.9(17)[b]
O–P–F	95.3(5)	96.0(5)	95.0(5)	98.3(6)
	93.2(6)	94.2(6)	96.8(5)	
F–P–F	97.6(6)	97.0(6)	95.7(6)	96.4(14)
O′–P′–O	111.5(5)	111.0(5)	111.3(5)	115.5(8)[c]

[a] These angles correspond to co-ordinates in Table 6. However, within each chain the hand of the molecules alternates. [b] True dihedral angle, calculated from twist angle (see Table 2) to allow comparison with crystal data. [c] Dependent parameter, not refined.

X-Ray Powder Diffraction Studies.—A sample sealed in a Pyrex capillary tube was mounted on an Enraf-Nonius Guinier-Simon powder camera equipped with a low-temperature device. As indicated by the single-crystal study, initial crystallisation gives the hexagonal form, which is stable for at least several days at temperatures down to the limit of our apparatus (*ca.* 100 K). However, on immersion in liquid nitrogen at 77 K the transformation to the trigonal form is complete within 5—10 min.

Table 8. Comparison of relevant structural parameters of $PO(OPF_2)_3$ with those of PF_3 and other OPF_2 compounds (distances in Å, angles in °)

Compound	r(P–F)	r(P–O)	F–P–F	O–P–F	Ref.
PF_3	1.570(1)	—	97.8(2)	—	3
$(PF_2)_2O$	1.570(5)	1.597(9)	98.5[a]	98.8(3)	4
$C_6H_5OPF_2$	1.582(16)	1.595(37)	98.0[a]	98.4(3)	5
1,4-$C_6H_4(OPF_2)_2$	1.577(7)	1.598(13)	96(3)	97.8(16)	6
1,3-$C_6H_4(OPF_2)_2$	1.581(6)	1.597(10)	97(2)	98.3(6)	6
CH_3OPF_2[b]	1.591(6)	1.560(20)	94.8(6)	102.2(10)	7
$PO(OPF_2)_3$	1.581(10)	1.576(25)	96.4(14)	98.3(6)	

[a] Fixed. [b] Microwave structure, values not strictly comparable.

Variable-temperature runs from 100 to 273 K showed no further phase changes for either form before melting: in particular, the trigonal form does not revert to the hexagonal on warming and the latter can be regenerated only by melting and recrystallisation of the sample. The melting points of the two modifications (261 K) are indistinguishable. From powder patterns recorded at 158 K (the data collection temperature for the single-crystal study) and calibrated against Si as an external standard, accurate unit-cell parameters were obtained as follows: trigonal form, a = 12.917 3(21), c = 9.261(4) Å, U = 1 338 Å^3; hexagonal form, a = 15.020(4), c = 9.208(6) Å, U = 1 799 Å^3.

Discussion

Gas-phase Structure.—A comparison of this structure with those of PF_3 and other OPF_2 compounds is shown in Table 8. The FPF angle in PF_3 is generally somewhat larger than in the difluorophosphines and slightly smaller than the OPF angle. This is as expected from consideration of the electronegativities of the substituents on phosphorus. The P–O distance found in this work is rather shorter than those in related compounds, but the difference is not significant. Overall, the values found here are in close agreement with those of the other structures.

The O–P′–O angle in $PO(OPF_2)_3$ [102.8(7)°] is not significantly different from that found in the gas-phase structure of $PO(OCH_3)_3$[18] [105.0(29)°] and is only slightly larger than the FPF angle in PF_3O[19] [101.3(2)°], as would be expected since oxygen is less electronegative than fluorine. The P′–O distances in $PO(OCH_3)_3$ and $PO(OPF_2)_3$ are also not significantly different from each other [1.580(2) and 1.590(9) Å]. The P′–O′ distance in $PO(OCH_3)_3$ [1.477(6) Å] is considerably longer than in $PO(OPF_2)_3$ [1.401(10) Å]. Furthermore, the more comparable P′–O′ distance in PF_3O [1.436(6) Å] is also significantly longer than that in $PO(OPF_2)_3$.

An interesting aspect of this structure is the close arrangement of three of the fluorine atoms, one in each PF_2 group. Although their separation (2.46 Å) is less than the sum of van der Waals radii for two fluorine atoms (2.7 Å), this distance may be subject to systematic error due to shrinkage effects, corrections for which were outside the scope of this work. Nevertheless there is clearly a very short fluorine–fluorine contact in the conformation which the molecule appears to adopt. Similar comments apply to the rather short P···O distances of 3.02 Å between the phosphorus atom in one OPF_2 group and the oxygen atom in an adjacent group.

When considering the conformation of this molecule it is, of course, important to consider the effect of lone pairs of electrons, particularly those on the phosphorus and oxygen atoms in the OPF_2 groups. From the evidence of the crystal structures of disiloxane[20] and methoxysilane[21] and electron diffraction studies of substituted disiloxanes[22] it seems probable that there is only one stereochemically active lone pair on the oxygen atom: the second pair of electrons is in a perpendicular p orbital. It seems reasonable to suppose a similar situation might exist for an oxygen atom bonded to two

Table 9. Significant intermolecular contacts A–B···C–D

A	B	C	D	Distance B···C (Å)	Angle A–B···C (°)	Angle B···C–D (°)
P(1)	O(1)	P(1)	O(1)	3.200(11)	180	180
P(1)	O(1)	P(2)	O(2)	2.906(12)	121.5(6)	77.2(4)
			F(1)			76.6(4)
			F(2)			168.1(6)
P(3)	O(3)	P(3)	O(3)	3.137(9)	180	180
P(3)	O(3)	P(4)	O(4)	2.868(9)	121.1(5)	76.6(4)
			F(3)			78.9(4)
			F(4)			169.3(5)
P(5)	O(5)	P(5)	O(5)	3.144(9)	180	180
P(5)	O(5)	P(6)	O(6)	2.894(9)	121.4(5)	75.6(4)
			F(5)			78.7(4)
			F(6)			170.0(5)

In each case, atoms C and D are in a molecule related by the c-glide operation to the molecule containing A and B.

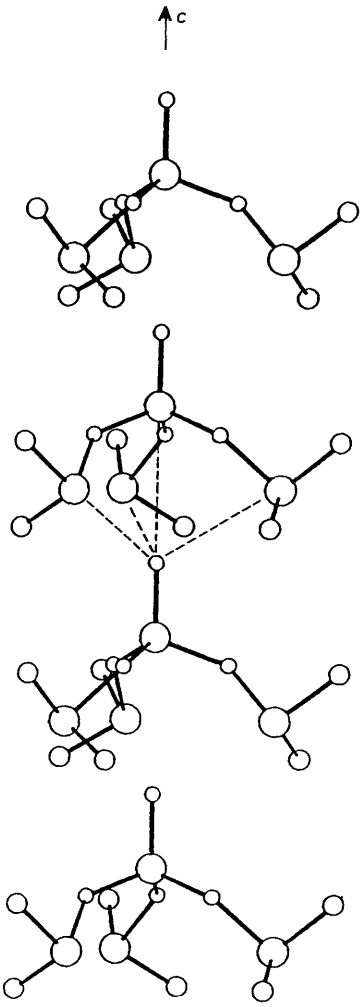

Figure 4. View of one chain of molecules running parallel to the crystallographic c axis. The short O···P intermolecular contacts are shown as dashed lines for one pair of molecules

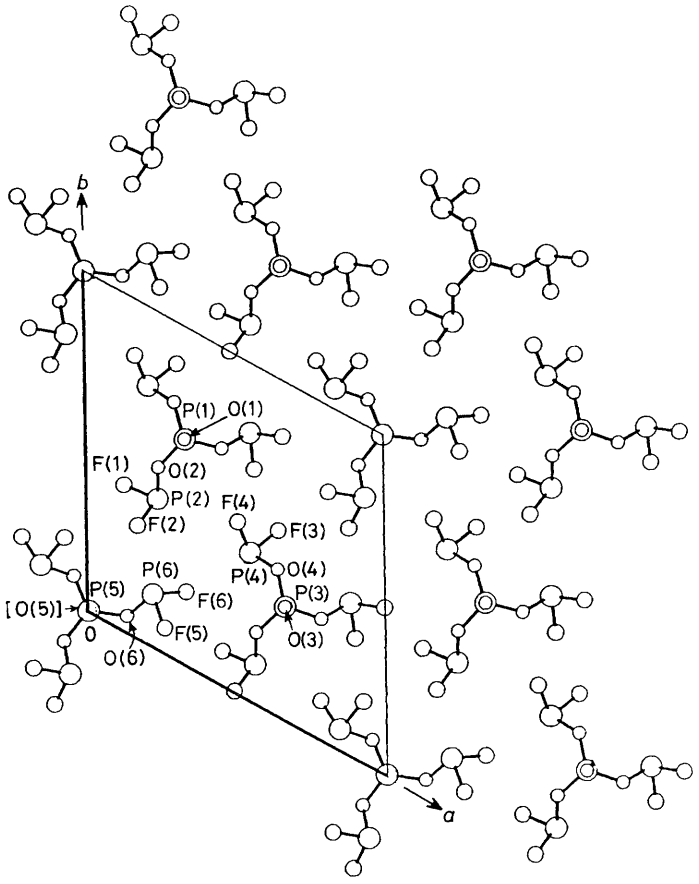

Figure 5. *c*-Axis projection of the crystal structure showing the relative disposition of the OPF_2 substituents and interlocking of fluorine atoms between neighbouring molecules

phosphorus atoms. If this is assumed to be the case then this lone pair on the oxygen atom is staggered with respect to the other oxygen atoms on the central phosphorus and this could largely explain the conformation here, in which the O–P bonds almost eclipse P′–O bonds. In each OPF_2 group the lone pair on the trivalent phosphorus atom is staggered with respect to the bond to the central phosphorus atom, but one of the P–F bonds eclipses the lone pair of electrons on the oxygen atom. However, the interactions of the phosphorus lone pair and the fluorine atoms with the oxygen atom in the neighbouring OPF_2 group are probably also important in determining the conformation here. If the P–O twist angle is increased the phosphorus and oxygen lone pairs become closer, while if it is considerably decreased one of the fluorine atoms approaches the oxygen atom too closely.

Solid-state Structure.—The crystallographic asymmetric unit comprises three independent one-third molecules. Each molecule lies on a crystallographic three-fold axis and thus has C_3 molecular symmetry.

The relative orientations of the molecules in the unit cell are rather unusual, with four molecules per cell parallel, and two anti-parallel, to the crystallographic *c* axis. Molecules related by *c*-glide plane operations are linked into linear chains by one close (3.14 Å), linear P′=O′ · · · P′ contact and three somewhat shorter (2.88 Å) P′=O′ · · · P contacts (Figure 4). For the reasons mentioned above, contacts involving P(1) and O(1) are slightly anomalous and will not be discussed further: however, they are listed in Table 9 which specifies the geometries of the significant intermolecular contacts. Each P′=O′ · · · P contact is approximately *trans* to one of the fluorine atoms on P: this confers a distorted trigonal bipyramidal environment on P, with O′ and one F axial and the equatorial plane occupied by the remaining F, O, and the P lone pair.

Unlike phosphine sulphides and selenides, phosphine oxides commonly pack head-to-tail with P=O vectors parallel: this is generally explained in terms of the alignment of the more polar P=O bonds, but the non-bonded O · · · P distances usually lie outside the sum of the van der Waals radii for O and P (3.3 Å): for example in $PO(CH_2CH_2CN)_3$ [23] the O · · · P separation is over 3.6 Å. In the case of $PO(OPF_2)_3$, the presence of the phosphorus atoms in the substituent chains appears to be crucial in allowing much closer approaches between molecules. Although there are no close contacts between chains of molecules, the dominant characteristic of the molecular packing in the *ab* plane lies in the relative dispositions of the OPF_2 substituents: a *c*-axis projection (Figure 5) shows the cog-like interlocking not only of the chains as a whole but also of individual fluorine atoms.

As we have been unable, as yet, to determine the crystal structure of the hexagonal phase, any explanation of the highly unusual topotactic nature of the hexagonal ⟶ trigonal transformation must remain rather speculative. However, the almost identical lengths of the *c* axes in the two forms suggest that both involve the linear P′=O′ · · · P′ chains seen in the trigonal modification. Large atomic displacements are inconsistent with a topotactic transformation; that is, the survival, intact, of the single crystal through the phase change. We

therefore suggest that the phases differ essentially in the disposition of the OPF_2 chains, such that the interlocking seen in the trigonal form is absent in the hexagonal: this would also explain why, once the crystal has adopted the more efficient packing in the trigonal form, the phase change is not reversible. We suspect that the transformation involves mainly rotation of the molecules about their three-fold axes and changes in the torsions about the P′–O and O–P bonds.

Comparison of Crystal and Gas-phase Structures.—Although there are differences in bond lengths and in valence angles between the molecules of $PO(OPF_2)_3$ in the crystal and those in the gas phase (Table 7), the most obvious contrast lies in the different torsion angles observed about the P–O single bonds. Disregarding the P′=O′ distance in molecule 1 of the crystal structure, since it appears to be strongly affected by residual disorder, the remaining P′=O′ distances of 1.482(9) and 1.475(9) Å are considerably longer than the gas-phase value of 1.401(10) Å, as might be expected in view of the relatively short P′=O′ • • • P′ intermolecular contact. The P–O distances in the crystal are all significantly longer than in the gas phase. They are also much longer than the P′–O distances in the crystal. A bond to a four-co-ordinate phosphorus(v) atom would normally be expected to be no more than 0.03 or 0.04 Å shorter than a similar bond to three-co-ordinate phosphorus(III), and the large differences between the phases are due to the presence of intermolecular P′=O′ • • • P contacts as described above.

The wider O–P′–O and P′–O–P angles in the crystal point to an overall flattening of the molecule compared with the gas phase (obviously, the narrower O′–P′–O angles are linked to the wider O–P′–O angles). There are no significant differences between the O′–P′–O–P dihedral angles observed in the two phases, but the P′–O–P–F dihedral angles differ by over 50°: this is attributable to a reorientation of the PF_2 group as a result of the close P′=O′ • • • P interactions. Again, the effect is to cause a flattening of the molecule: even with the extension of the P′=O′ bond in the crystal, the length of the molecule in the direction parallel to that bond is only 3.89 Å in the solid state compared with 4.45 Å in the gas phase. This flattening of the molecule also causes an increase in its radius (the distance, in the *xy* plane, of the furthest atom from the C_3 axis) from 3.46 Å in the gas phase to 3.78 Å in the crystal.

Acknowledgements

We thank the S.E.R.C. for financial support.

References

1 E. R. Cromie, G. M. Hunter, and D. W. H. Rankin, *Angew. Chem., Int. Ed. Engl.*, 1980, **19**, 316.
2 G. M. Hunter, Ph.D. Thesis, Edinburgh University, 1981.
3 T. Moritani, K. Kuchitsu, and Y. Morino, *Inorg. Chem.*, 1969, **8**, 867.
4 D. E. J. Arnold and D. W. H. Rankin, *J. Fluorine Chem.*, 1972, **2**, 205.
5 A. M. Marr, Ph.D. Thesis, Edinburgh University, 1988.
6 G. A. Bell, D. W. H. Rankin, and H. E. Robertson, *J. Mol. Struct.*, in the press.
7 E. G. Codding, C. E. Jones, and R. H. Schwendman, *Inorg. Chem.*, 1974, **13**, 178.
8 C. M. Huntley, G. S. Laurenson, and D. W. H. Rankin, *J. Chem. Soc., Dalton Trans.*, 1980, 954.
9 S. Cradock, J. Koprowski, and D. W. H. Rankin, *J. Mol. Struct.*, 1981, **77**, 113.
10 A. S. F. Boyd, G. S. Laurenson, and D. W. H. Rankin, *J. Mol. Struct.*, 1981, **71**, 217.
11 L. Schäfer, A. C. Yates, and R. A. Bonham, *J. Chem. Phys.*, 1971, **55**, 3055.
12 A. J. Blake, S. Cradock, E. A. V. Ebsworth, D. W. H. Rankin, and A. J. Welch, *J. Chem. Soc., Dalton Trans.*, 1984, 2029.
13 SHELX 84, G. M. Sheldrick, University of Göttingen, 1983.
14 SHELX 76, G. M. Sheldrick, University of Cambridge, 1976.
15 CALC, R. O. Gould and P. Taylor, University of Edinburgh, 1985.
16 ORTEP II, interactive version, P. D. Mallinson and K. W. Muir, *J. Appl. Cryst.*, 1985, **18**, 51.
17 PLUTO, W. D. S. Motherwell, University of Cambridge, 1976.
18 H. Oberhammer, *Z. Naturforsch., Teil A*, 1973, **28**, 1140.
19 T. Moritani, K. Kuchitsu, and Y. Morino, *Inorg. Chem.*, 1971, **10**, 344.
20 M. J. Barrow, E. A. V. Ebsworth, and M. M. Harding, *Acta Crystallogr., Sect. B*, 1979, **35**, 2093.
21 A. J. Blake, M. Dyrbusch, E. A. V. Ebsworth, and S. G. D. Henderson, *Acta Crystallogr., Sect. C*, 1988, **44**, 1.
22 D. W. H. Rankin and H. E. Robertson, *J. Chem. Soc., Dalton Trans.*, 1983, 265.
23 A. J. Blake, R. A. Howie, and G. P. McQuillan, *Acta Crystallogr., Sect. B*, 1981, **37**, 997.

Received 26*th February* 1988; *Paper* 8/00883C